Demonstration of Mobile Fronthaul Test Bed Based on RoF Technology Supporting Two Frequency Assignments and 2 × 2 MIMO Antennas

Seung-Hyun Cho, Changyo Han, Hwan Seok Chung, and Jong Hyun Lee

We demonstrate a next-generation high-capacity mobile fronthaul based on radio over fiber (RoF) technology, which links between a digital unit and a radio unit supporting two frequency assignments and 2 × 2 multiple input, multiple output antennas. To confirm the technical feasibility of a mobile fronthaul, we experimentally investigate its down- and uplink end-to-end performances including the optical and radio frequency (RF) signal path. Frequency-dependent performance deviations, error vector magnitude variations, overall system performance variations caused by optical to electrical conversion, and intermediate frequency to RF conversions are examined. Experimental verifications on multiple LTE uplink signals are performed for the first time. We also demonstrate several commercial mobile Internet services, YouTube video streaming, and file transfers using off-the-shelf mobile devices, through a mobile fronthaul based on RoF.

Keywords: Mobile fronthaul, LTE, RU, DU, RoF, C-RAN.

Manuscript received Feb. 23, 2015; revised July 22, 2015; accepted Sept. 4, 2015.

This work was supported by the IT R&D programs of MSIP (Ministry of Science, ICT and Future Planning), Rep. of Korea (15ZI1310, Development of compact radio & dense digital base station technologies based on RoF for mobile communication systems).

Seung-Hyun Cho (corresponding author, shc@etri.re.kr), Changyo Han (hanc@etri.re.kr), Hwan Seok Chung (chung@etri.re.kr), and Jong Hyun Lee (jlee@etri.re.kr) are with the Communications Internet Research Laboratory, ETRI, Daejeon, Rep. of Korea.

I. Introduction

The global mobile Internet market has recently exploded in growth through the rapid progress of broadband wireless communication technologies [1]. As a result, the development of broadband mobile Internet services has increased the total amount of traffic handled by the existing base stations for mobile communications; consequently, this has led to a growth in spending for the installation and maintenance of *mobile* base stations [2]. These phenomena have brought about structural changes in *legacy* mobile base stations, in which digital signal processing units and remote radio signal processing units are divided functionally, and are separately operated and maintained to reduce telecom operator expenditures. We call this separate configuration a cloud or centralized radio access network (C-RAN) architecture [3].

Until now, an optical link has been used between a digital unit (DU) and radio unit (RU), which is known as a *mobile fronthaul* employing a digital optical communication method based on interfacing technologies such as the common public radio interface (CPRI)/open radio base station architecture initiative in C-RAN [4]–[5]. However, the problem of bandwidth shortage in previous mobile fronthauls has been an issue, because of an increase in the traffic handling capacity per mobile base station caused by a rapid evolution of the recent ultra-broadband mobile telecommunication system. For instance, it is necessary to accommodate approximately 20 Gbps of digital data traffic in the current mobile fronthaul configuration based on the CPRI technique for supporting one RU with two frequency assignments (FAs), three sectors, and 4 × 4 MIMO antennas [6]. If a DU supports multiple RUs through the current mobile fronthaul simultaneously, then it will require additional digital data traffic. Therefore, most service providers will spend a huge amount of money on the installation and maintenance of their infrastructure. As a result, they will give up installing their next-generation mobile fronthaul link or put their subscribers to the entire expense of setting up a mobile base station.

There have been several attempts to solve these technical and economic issues caused by the aforementioned excessive traffic growth. First, in-phase and quadrature phase (I and Q) sample compression techniques have been proposed and realized in current mobile fronthaul systems [7]. Owing to the invention of various kinds of compression techniques, we were able to reduce the total traffic volume of mobile fronthaul by more than 30% [8]. The second method is a proper separating technology between the physical layer and media access control layer in the DU to minimize the total handling traffic capacity in a mobile fronthaul [9]. Finally, a newly defined mobile fronthaul architecture based on an analog radio over fiber (RoF) technique has begun to be more intensively researched for realization of an ultra-high-capacity next-generation mobile communication system [10]–[12].

Several research groups have researched and developed a mobile fronthaul using the intermediate frequency over fiber (IFoF) technique, which is a typical RoF technology [6], [11]–[14]. In an IFoF transmission system, multiple radio signals can be allocated, up to as many as the number of intermediate frequencies (IFs), within a particular bandwidth. Compared to a digitized signal transmission, it is not necessary to utilize the relatively larger bandwidth caused by data sampling procedures. Caballero and others successfully demonstrated 12 subcarriers with 100 Mbaud and 16 QAM in a 150 MHz frequency grid on a single optical carrier using phase modulation [13]. The transmission characteristics of multi-IF carriers with an LTE baseband signal were also mathematically investigated in [11]. Most of the previous investigations were mainly focused solely on the performance of the optical transmission [15]–[18].

In this paper, we implement an RoF-based mobile fronthaul test bed composed of a DU, an analog optical link, and an RU. The DU is configured with a software platform–based LTE base station, and the RU is also constituted to support two FAs and 2 × 2 MIMO antennas. To link between the DU and RU, a mobile fronthaul optical link based on an analog RoF technique is realized to support a C-RAN with two FAs, one sector, and 2 × 2 MIMO antennas. Experimental verifications on multiple LTE uplink and downlink signals including the whole end-to-end data path from the DU to RU are made for the first time. We also demonstrate several commercial mobile Internet services (such as Skype), YouTube video streaming, and file transfers using off-the-shelf mobile devices, including smartphones and tablet computers, through a mobile fronthaul based on RoF. In Section II, we introduce the detailed mobile fronthaul architecture and describe its specific operating principles. The signal flows from the DU to the RU and vice versa are also described. We investigate the downlink performances throughout the whole optical link and radio frequency (RF) signal path in Section III. In Section IV, the upstream transmission performances are also verified for various kinds of operating conditions. In Section V, a few system demonstration results, such as the throughput analysis and SNR measurement using a DU platform, are presented. Finally, some concluding remarks are provided in Section VI.

II. System Architecture

In Fig. 1(a), a cost-effective mobile fronthaul architecture based on analog RoF technology is illustrated. We basically employ two types of multiplexing methods — wavelength division multiplexing (WDM) and frequency division multiplexing (FDM) — in this configuration to maximize the link capacity and cost efficiency. In principle, a single DU can be connected to multiple RUs. For physical connection between RUs and a DU, we utilize a few tens of frequencies or wavelengths. Thus, the total number of wireless baseband signals supported by this mobile fronthaul is given by $N \times M/2$, where N is the number of accommodated frequencies at a single wavelength and M is the number of wavelengths to be employed. The denominator indicates the separation of upstream and downstream transmissions by different wavelengths. As shown in Fig. 1(a), we employ a ring-type architecture as a physical link topology. Most telecom operators prefer this ring topology to other kinds of configurations owing to its high level of survivability, which is due to the fact that it can be easily protected and restored.

The detailed operating principle of generating and detecting mobile communication signals at the DU and RU is shown in Fig. 1(b). For a downstream transmission from the DU to RU, multiple baseband signals from baseband modems are aggregated and the DU is modulated onto any predefined IF carrier and then digital-to-analog converted. Each converted signal is directly modulated with a distributed feedback laser diode (DFB-LD) and transmitted to the RU throughout a single-mode fiber (SMF). In the RU, an optical signal is converted to an electrical signal by an optical receiver. The converted signal is then divided, filtered, and separated by each IF carrier frequency. After the frequency up-conversion process,

http://dx.doi.org/10.4218/etrij.15.0115.0146

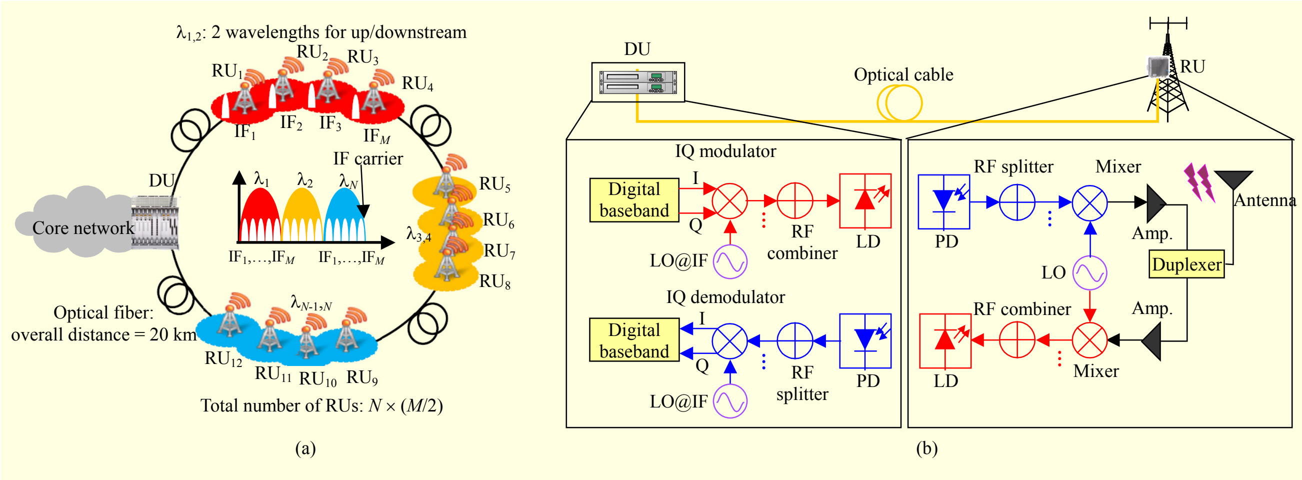

Fig. 1. (a) Cost-effective mobile fronthaul architecture based on analog RoF technology and (b) detailed operating principle of generating and detecting mobile communication signals at DU and RU.

each converted RF signal in a licensed band is transmitted over the air through high-power amplifiers and antennas.

An upstream signal proceeds in the reverse direction as a downstream signal. Each upstream signal generated from a subscriber's equipment is transmitted to antennas located at the RU. Signals arriving at the antenna are frequency down-converted after passing through low noise amplifiers (LNAs). Multiple frequency down-converted signals are combined in the frequency domain and then directly modulate a DFB-LD before finally being transmitted to the DU over an SMF. First, signals arriving at the optical front-end of the DU are optically-to-electrically converted using an analog optical receiver. Mobile upstream signals are then detected and demodulated in the digital signal processor at the DU after being converted into a digital signal passing through an analog-to-digital converter (ADC).

III. Experimental Results of Downlink

In Fig. 2, the detailed experimental setup to examine the downstream transmission performances is shown. We employed an LTE base station (LTE-100™) based on a software platform manufactured by Amarisoft™ as a DU directly connected to the core network. This LTE base station provides the full function of an evolved packet core and partial function of an Evolved Node B. In the DU-RoF interfacing equipment, each downstream I/Q signal generated at the DU is mapped onto a specific IF carrier and then converted into an analog signal for a proper analog optical transmission. The output of the DU-RoF interfacing equipment is multiple wireless baseband signals with an analog waveform multiplexed in the frequency domain. Thus, the output of the DU-RoF interfacing equipment in the downstream direction is used for driving the directly modulated laser diode. In the RoF-Tx, a cooled analog DFB-LD module with a modulation bandwidth of up to 3 GHz, manufactured by Emcore™, was utilized as a directly modulated light source. The emission wavelength of the LD was 1,548.5 nm, and its output power was about +2.5 dBm (the operating current was 22 mA). We intentionally chose this operating current/output power condition to obtain an approximately 10% optical modulation index (OMI)/channel with a fixed output level of the DU-RoF interfacing equipment, which was previously reported in [10].

Downstream light with frequency multiplexed mobile communication signals from an RoF-Tx was transmitted over SMF. In this experiment, we chose a dual-fiber unidirectional transmission scheme to avoid single-fiber bidirectional transmission–induced interference. The downstream signal was electrically converted by the RoF-Rx at the RU. This electrical signal was frequency up-converted from the IFs into RFs after being separated by the IF throughout the electrical splitter and bandpass filter. We adopted the LTE band-7 frequency plan. Thus, electrically converted signals centered at 150 MHz and 270 MHz were converted into RF signals centered at 2,660 MHz for both Antenna-1 and Antenna-2. Similarly, downstream signals located at 170 MHz and 290 MHz were also converted into 2,680 MHz. Finally, all frequency up-converted downstream signals were transmitted over the air again.

The IF plan employed in the experiment is shown in the inset of Fig. 2. To support a mobile fronthaul with two FAs and two MIMO antennas, four IF carriers with a 20 MHz bandwidth were utilized in the experimental setup. The channel spacing of the IF for the two antennas was set to 120 MHz. There was no frequency spacing between the two signals for the FA to add and drop the adjacent IF signals easily. Owing to

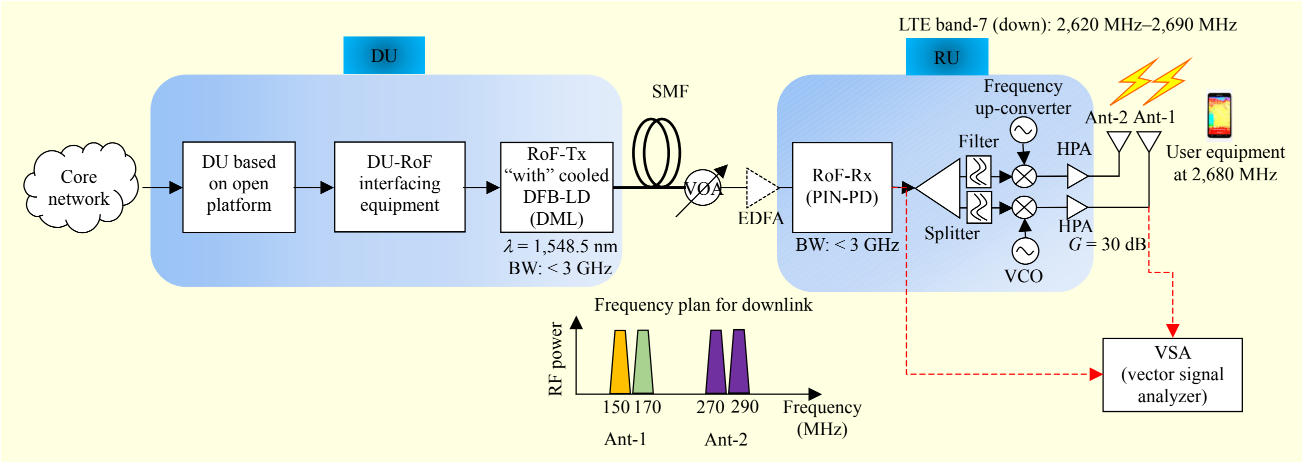

Fig. 2. Experimental setup for downlink.

the orthogonality of the LTE signals, there was no interference-induced signal degradation. As shown in the inset of Fig. 2, we employed an LTE signal centered at 170 MHz as an upstream-and-downstream channel for practical mobile Internet services. Aside from this channel, three kinds of 64 QAM mapped LTE-OFDM signals based on LTE downlink test model 3.1 (E-TM 3.1) were used as dummy channels.

In Fig. 3(a), the measured electrical spectrum of a downstream signal at the output of the DU-RoF interfacing equipment is shown. There were some spikes owing to the insufficient bit resolution of the DAC employed for the DU-RoF interfacing equipment [11]. The peak at 10 MHz was the reference frequency for the up/down conversion. As shown in Fig. 3(a), there was an unoccupied LTE-OFDM spectrum located at 170 MHz because the subscriber did not require downstream traffic with a high bandwidth when using this IF channel. To support an RU with two FAs and 2 × 2 MIMO antennas, four IF carriers with a carrier-to-noise ratio (CNR) of more than 50 dB were obtained.

The RF spectrum of the downstream signal measured at the RU (Antenna-1) is shown in Fig. 3(b). We were able to see two kinds of LTE-OFDM signals within the LTE frequency band-7 spectrum, which were composed of a dummy signal based on E-TM 3.1 and a practical mobile Internet service channel, respectively [19].

Table 1 shows measured error vector magnitude (EVM) values and channel power values of a downstream signal at different IF carrier frequencies. Overall, the frequency-dependent channel characteristics of the downstream signal were maintained even when the signal passed through various kinds of devices, such as multiple-stage RF amplifiers, frequency up-converters, optical transceivers, and an SMF. From a statistical point of view, it is worth noting that the optical-to-electrical conversion process degraded the EVM by 0.5%, and the frequency up-conversion and power

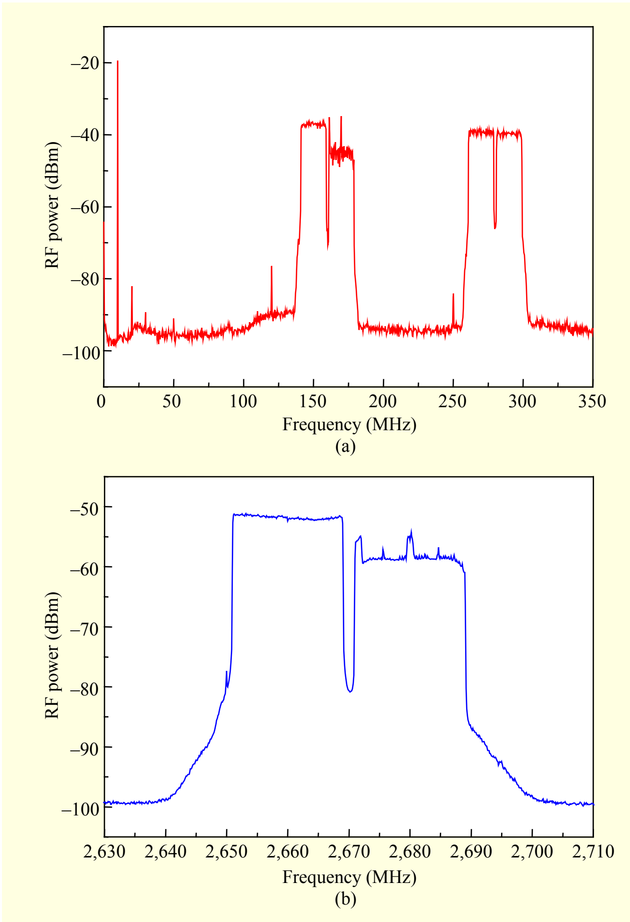

Fig. 3. (a) Measured electrical spectrum at output of RoF-Rx and (b) measured electrical spectrum at output of Antenna-1 of RU.

amplification process degraded the EVM by 0.5%.

Figure 4 shows the measured EVM of a downstream signal at the output of the RoF-Rx and that of Antenna-1 of the RU by varying the optical received power. The measured EVM values at the output of the RoF-Rx gradually increase when

http://dx.doi.org/10.4218/etrij.15.0115.0146

Table 1. Measured EVM values and channel power values of downstream signal at different IF carrier frequencies.

IF frequency (MHz)	Output of DU-RoF interfacing equipment		RoF-Rx		Output of Ant-1/Ant-2		RF frequency (MHz)	Note
	Power (dBm)	EVM (%)	Power (dBm)	EVM (%)	Power (dBm)	EVM (%)		
150	–9.7	0.7	–15.5	1.25	–0.36	1.77	2,660	Ant-1
170	N/A	N/A	N/A	N/A	N/A	N/A	2,680	Ant-1
270	–11.7	1.15	–17.3	1.7	–2.5	2	2,660	Ant-2
290	–12.1	1.2	–18	1.85	–3.3	2.22	2,680	Ant-2

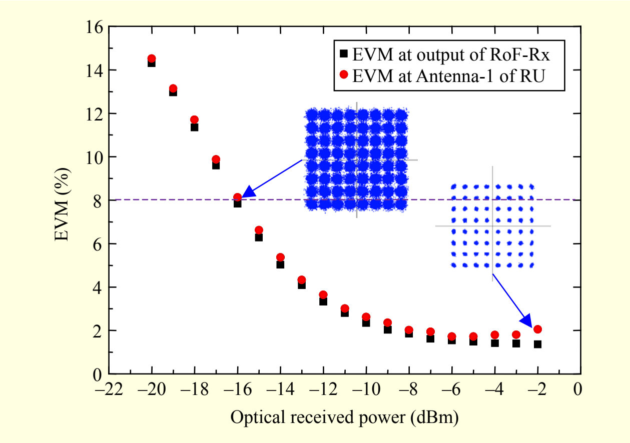

Fig. 4. Measured EVM of downstream signal at output of RoF-Rx, and that of Antenna-1 of RU.

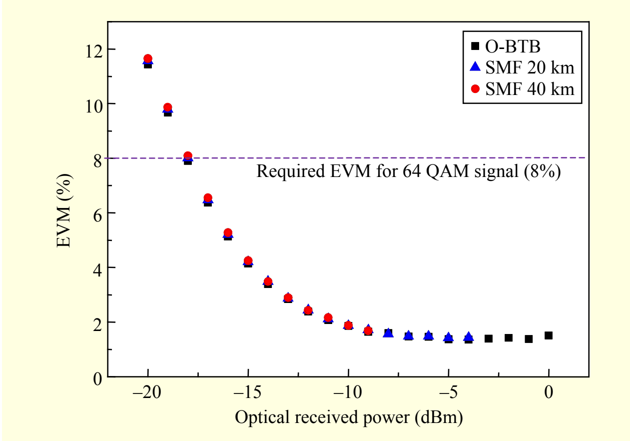

Fig. 5. Measured EVM values at different fiber lengths.

decreasing the optical received power, as we can easily expect. The measured downlink performances at the antenna illustrate EVM degradations caused by a frequency up-conversion and high power amplification process. We measured all EVM values of the downstream signal centered at 270 MHz. As illustrated in Fig. 4, we concluded that the optical received power for the RoF-Rx should be more than –17 dBm to satisfy an EVM of 8%, which is the minimum requirement of the 3rd Generation Partnership Project (3GPP) [20]. Otherwise, EVM degradations were also observed because of the saturation characteristics of a high power amplifier (HPA) at the input of the antenna when the received optical power was increased from –5 dBm to –2 dBm. As a result, it should be noted that an automatic input level controller at the input of the HPA is needed to achieve the best EVM performance of a downstream RF signal over the air. The measured 64 QAM constellations for a downstream signal at the output of the antenna are also shown in the inset of Fig. 4, when the received optical power was set to –2 dBm and –17 dBm, respectively.

In Fig. 5, the measured EVM values at different fiber lengths are also depicted for when we employed similar measurement conditions, as described in Fig. 4. There were no observable EVM differences owing to the relatively narrower bandwidth of an LTE-OFDM downstream signal of 20 MHz when increasing the fiber distance to up to 40 km.

Measured EVM values of the downstream mobile signals for changing the optical path loss are also shown in Fig. 6. To measure the EVM, we also investigated the downstream signal centered at 270 MHz. As we have already shown in Fig. 4, there were slight EVM variations caused by a frequency up-conversion and high power amplification process without using an optical amplifier. In this experiment, we employed a single-stage erbium-doped optical fiber amplifier (EDFA) operated in automatic current control mode. We fixed the driving current at 70 mA for the pump LD in the EDFA. However, the measured EVMs of the downstream signal were more slightly degraded (approx. 2%) when we utilized the optical amplifier. This is because optically-to-electrically converted amplified spontaneous emission (ASE) noise generated from the EDFA reduced the total CNR of a downstream signal. Not surprisingly, there was no significant EVM variation when the optical path loss was set to low (below 10 dB) when we employed the EDFA [21]–[22].

On the other hand, we saw observable EVM degradations caused by deteriorated noise figure characteristics of the EDFA

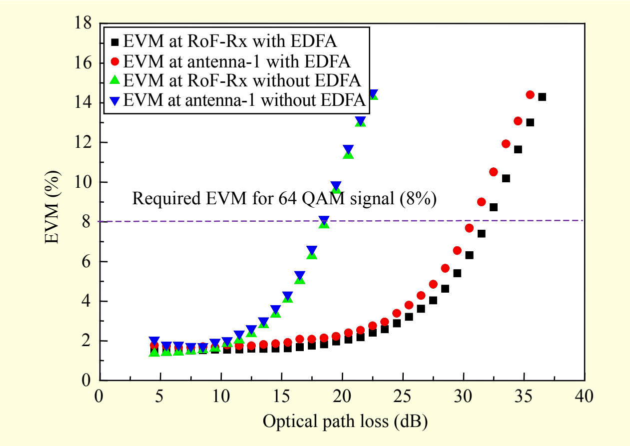

Fig. 6. EVM values of downstream mobile signal for changing optical path loss with and without using EDFA.

owing to the gain when increasing the optical path loss. We were able to obtain a total downlink power budget of 18 dB without using the EDFA, and 36 dB with the EDFA, to satisfy the minimum EVM requirement of 8% based on the 3GPP specifications. The power budget improvement was about 18 dB, which was directly related with the insertion loss of a commercialized 1 × 32 optical power splitter. By installing an EDFA as a preamplifier in the optical front-end of the RU, it is possible to share the optical infrastructure with current passive optical networks.

IV. Experimental Uplink Results

Figure 7 shows the detailed experimental setup to investigate the uplink performances. The RU was usually composed of antennas, LNAs, a frequency down-converter, an electrical (RF) combiner, a filter, and an RoF-Tx (analog optical transmitter) (see Fig. 7). Upstream signals within the LTE frequency band-7 were received by an antenna, and then amplified by the LNA with the proper gain for adequate analog signal processing. Multiple amplified signals are frequency down-converted to be suitable for an analog optical transmission based on the IFoF technique. Frequency-converted signals are combined by the RF combiner in the frequency domain. After the combiner, the signal can be amplified or attenuated to obtain the optimized OMI for an upstream optical transmission. For convenience, we employed a vector signal generator (VSG: SMW-200 manufactured by Rohde-Schwarz) as an upstream mobile signal source instead of using a common user equipment. As described in Section III, we also utilized the cooled analog DFB-LD module with a modulation bandwidth of up to 3 GHz as a directly modulated light source in the RoF-Tx. The center wavelength of our RoF-Tx was 1,548.5 nm. The output power of the transmitter was varied from +2.5 dBm to +5 dBm, which means that the operating current of the LD was increased from 22 mA to 36 mA. Practically, it has been very difficult to optimize the OMI and obtain better upstream transmission performances, because the power level of each upstream signal arriving at an antenna in the RU was different in the time domain. Therefore, we varied both the operating current of the LD and the input RF power into the LD to experimentally verify the impact of the received RF power at the antenna on the optical uplink performances. Electrical-to-optical converted upstream light with a multiplexed IF carrier was transmitted over SMF. In our experiment, we employed two fiber unidirectional transmission schemes; thus, the emission wavelengths of the RoF-Tx for the uplink and downlink were the same. Upstream light was electrically converted at the RoF-Rx at the DU. Electrical signals were converted into digital baseband signals using an

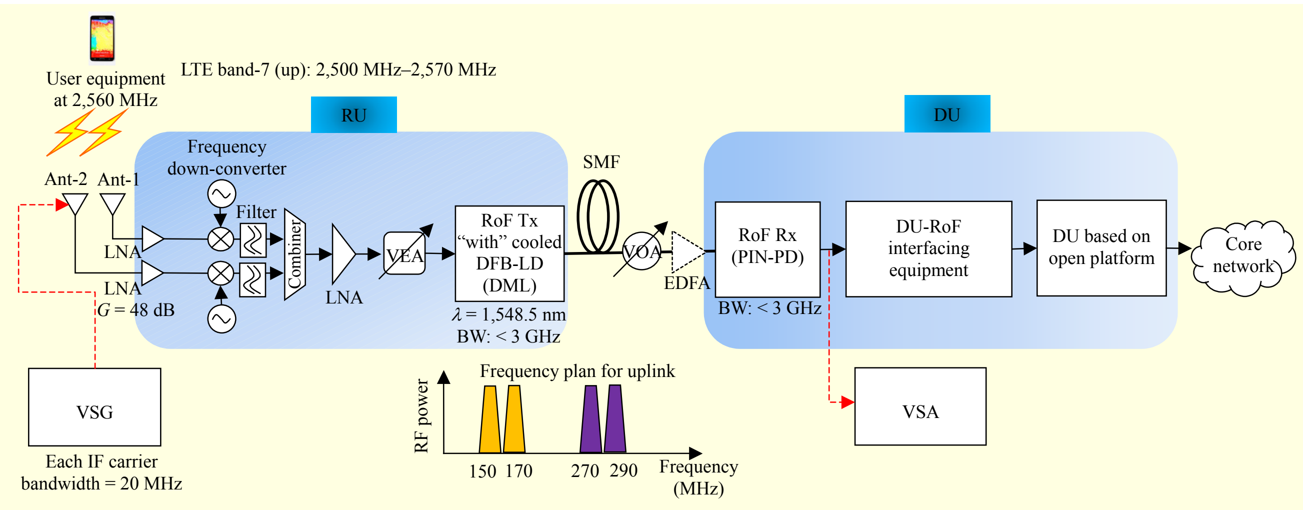

Fig. 7. Experimental setup for uplink.

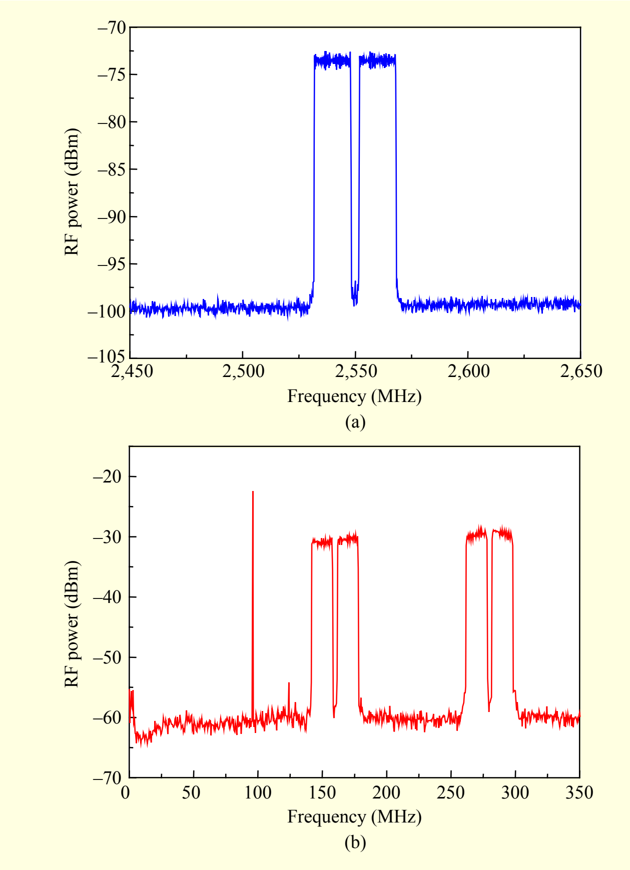

Fig. 8. Measured spectrum of upstream signal at (a) input of Antenna-1 of RU and (b) output of RoF-Rx in DU.

ADC and a digital IQ demodulator in the DU-RoF interfacing equipment to be suitable for digital signal processing. Finally, these digitally converted upstream IQ signals were demodulated and retransmitted to the core network in the LTE base station (LTE-100) based on a software platform made by Amarisoft™.

In Fig. 8, we show some of the measured spectrum of the upstream signal at different points. The upstream signal generated from the VSG, is shown in Fig. 8(a), which is the input signal at Antenna-1 and Antenna-2 of the RU. We generated two FA upstream signals with a 20 MHz bandwidth and LTE resource blocks (90 in each), which were centered at 2,540 MHz and 2,560 MHz, respectively [21]. In Fig. 8(b), we also describe the detailed frequency plan in the optical domain. We measured this spectrum at the output of the RoF-Rx at the DU. Similar to the downlink configuration, we employed four IF carriers with 20 MHz bandwidth supporting two FAs and two MIMO antennas for examining the upstream transmission performances. The frequency spacing between the IF carriers for multiple antennas was 120 MHz. The upstream signal centered at 96 MHz was employed to transmit the status monitoring information of the RU to the DU (see Fig. 8(b)).

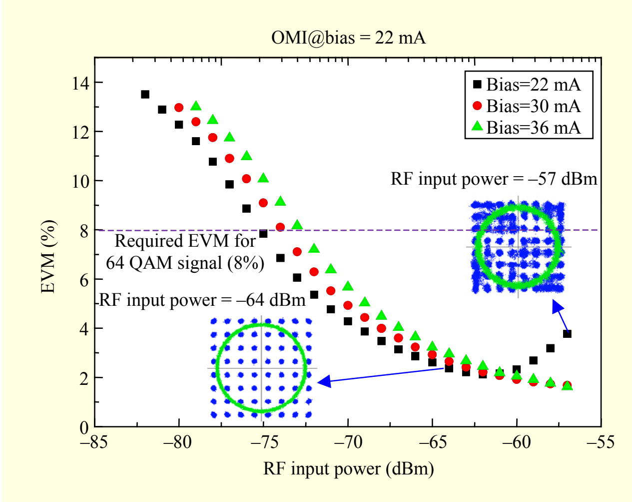

Fig. 9. Measured EVM values of upstream signal for varying input RF power to antenna at different bias current of LD in RoF-Tx.

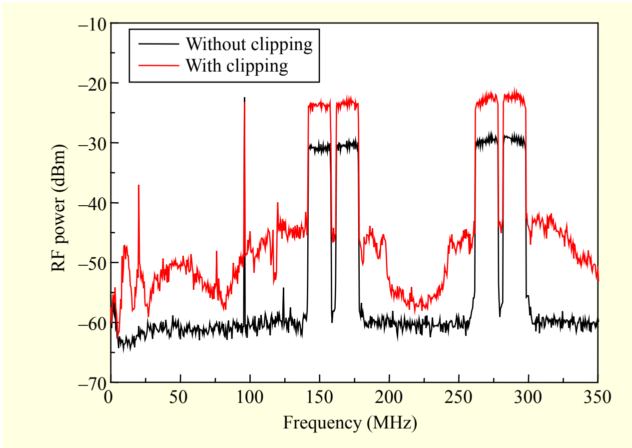

Fig. 10. Measured spectra of upstream signal with and without clipping phenomenon.

In Fig. 9, the measured EVM values of the upstream signal for varying the input RF power to the antenna at a different bias current of the LD in the RoF-Tx are shown. We also show the approximated OMI/channel value in the top axis of Fig. 9, when we set a bias current of 22 mA. The best optimal input RF power level was –62 dBm when we fix the bias current at 22 mA. When increasing the input power level from –62 dBm, EVM degradation caused by LD clipping was observed. When the transmission performances are degraded by LD clipping, the point of constellation at the edge regime is distorted in the constellation diagram, which is clearly shown in the inset of Fig. 9.

Meanwhile, there were still more chances to increase the OMI/channel when the bias current was set to above 30 mA. Because there is no chance to receive an upstream signal power level greater than –55 dBm in the real fields, it is very difficult

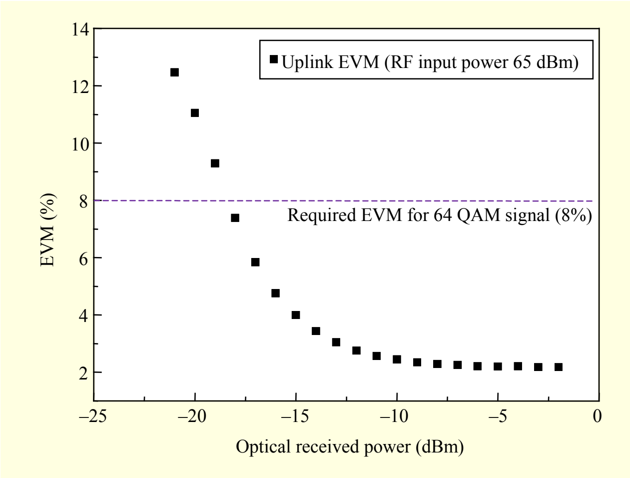

Fig. 11. Measured EVM variations for decreasing received optical power at RoF-Rx in DU.

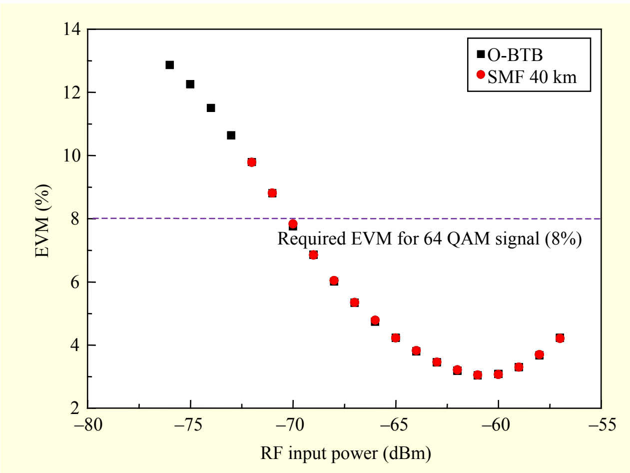

Fig. 12. Measured EVM of upstream signal at different fiber lengths.

to maximize the upstream transmission performances throughout the optimization procedure of the OMI/channel. Figure 10 also shows a spectrum of the upstream signal with and without the clipping phenomenon to verify the main reason for the EVM degradation shown in Fig. 9.

In Fig. 11, we illustrate the EVM variations for decreasing the received optical power at the RoF-Rx. We measured the EVM of the electrically converted signal whose carrier frequency was 270 MHz. To meet the minimum EVM requirement of 8% proposed by 3GPP, the received optical power should be higher than –18 dBm, which is a similar result described in the downlink experimental results.

We also present the measured EVM of the upstream signal at different fiber lengths, which is shown in Fig. 12. Similar to the results of the downlink, there was no significant EVM change when increasing the length of the SMF up to 40 km.

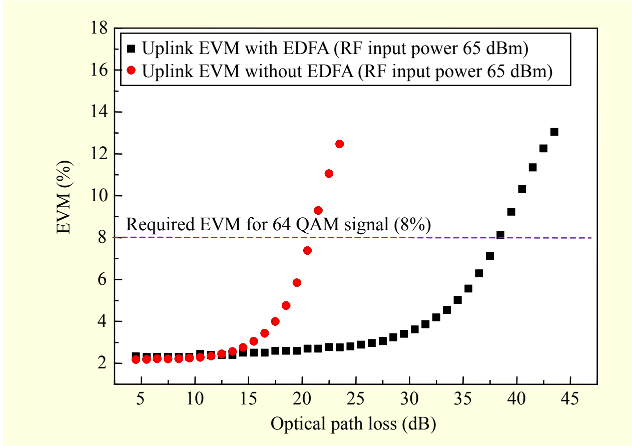

Fig. 13. Measured EVM of upstream signal at different optical path losses.

In Fig. 13, we also plot the measured EVM of the upstream signal centered at 270 MHz when varying the optical path loss. The RF input power level was fixed at –65 dBm for the measurements. The overall link power budget can be improved more than 80 times in the linear scale using an EDFA as a preamplifier. Consequently, we could obtain an uplink budget of 18 dB without using an EDFA, and 37 dB with an EDFA to satisfy the minimum EVM requirement of 8% based on the 3GPP specifications [21]. Thus, it should be noted that the link budget will be improved with the help of an optical amplifier.

V. System Demonstration

Figure 14(a) shows a photograph of the demonstrated mobile fronthaul test bed based on RoF technology. We were able to demonstrate two current mobile Internet services, Skype and YouTube video streaming, using three types of commercial mobile devices (see Fig. 14(b)). The measured data throughput and signal-to-noise ratio (SNR) of each channel offered by the DU platform (LTE-100 platform made by Amarisoft$^{\text{TM}}$) are depicted in Fig. 15. We obtained an uplink SNR from 10 dB to 20 dB for each user equipment, and approximately a 17 Mbps upload rate. Accordingly, we successfully confirmed that it can be possible to provide commercial LTE mobile Internet services in the C-RAN test bed, which was comprised of a DU, RU supporting two FAs, 2 × 2 MIMO antennas, and an RoF-based mobile fronthaul over an SMF of 20 km.

VI. Conclusion

We demonstrated a mobile fronthaul test bed consisting of a DU, an optical link, an RU, and a wireless link. The DU was implemented using a software platform, and the RU was

http://dx.doi.org/10.4218/etrij.15.0115.0146

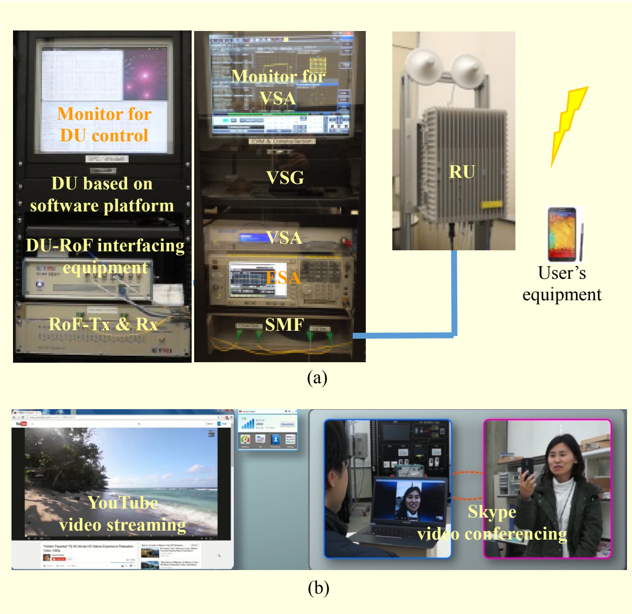

Fig. 14. Photographs of (a) our implemented test bed for mobile fronthaul based on RoF technology and (b) example of mobile Internet service.

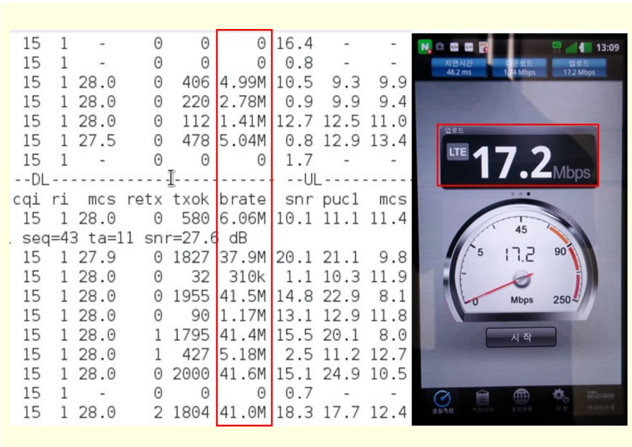

Fig. 15. Measured down and uplink data throughput and SNR of DU platform.

configured to support two FAs and 2 × 2 MIMO antennas. In the mobile fronthaul test bed based on the RoF technique, the down and uplink performances were qualitatively analyzed for achieving better transmission performances. We also examined all down and uplink performance degradations over the optical link and electrical RF path. Commercial mobile Internet services were successfully demonstrated using off-the-shelf mobile devices including a smartphone and tablet computer. From our analysis and demonstrated results, we expect that a cost-effective high-capacity mobile fronthaul for multiband LTE and 5G mobile services will be realized in the near future.

References

[1] C.L. I et al., "Toward Green and Soft: A 5G Perspective," *IEEE Commun. Mag.*, vol. 52, no. 2, Feb. 2014, pp. 66–73.

[2] J. Rasi et al., "Joint Compensation of Transmitter and Receiver IQ Imbalance in OFDM Systems Based on Selective Coefficient Updating," *ETRI J.*, vol. 37, no. 1, Feb. 2015, pp. 43–53.

[3] C.L. I et al., "Recent Progress on C-RAN Centralization and Cloudification," *IEEE Access*, vol. 2, Aug. 2014, pp. 1030–1039.

[4] CPRI Specification V6.0, *Common Public Radio Interface (CPRI);Interface Specification*, 2013.

[5] OBSAI, *Open Base Station Architecture Initiative BTS System Reference Document Version 2.0*, 2006.

[6] S.-H. Cho et al., "Cost-Effective Next Generation Mobile Fronthaul Architecture with Multi-IF Carrier Transmission Scheme," *Opt. Fiber Commun. Conf.*, San Francisco, CA, USA, Mar. 9–13, 2014, pp. Tu2B.6.

[7] N. Shibata et al., "Dynamic Compression Method Using Wireless Resource Allocation for Digitized Radio over TDM-PON System," *Opt. Fiber Commun. Conf.*, San Francisco, CA, USA, Mar. 9–13, 2014, pp. 1–3.

[8] B. Guo et al., "LTE/LTE-A Signal Compression on the CPRI Interface," *Bell Labs Techn. J.*, vol. 18, no. 2, Sept. 2013, pp. 117–133.

[9] NGMN, *Suggestions on Potential Solutions to C-RAN by NGMN Alliance V 4.0*, Frankfurt, Germany, Jan. 2013.

[10] S. Lee, S.-H. Cho, and J.H. Lee, "Future-Proof Optical-Mobile Converged Access Network Based on Integration of PON with RoF Technologies," *Int. Topical Meeting Microw. Photon. APMP*, Sapporo, Japan, Oct. 20–23, 2014, pp. 409–411.

[11] H.S. Chung et al., "Design of RoF Based Mobile Fronthaul Link with Multi-IF Carrier for LTE/LTE-A Signal Transmission," *Int. Topical Meeting Microw. Photon. APMP*, Sapporo, Japan, Oct. 20–23, 2014, pp. 303–306.

[12] S.-H. Cho et al., "Experimental Demonstrations of Next Generation Cost-Effective Mobile Fronthaul with IFoF Technique," *Opt. Fiber Commun. Conf.*, Los Angeles, CA, USA, Mar. 22–26, 2015, pp. 1–3.

[13] A. Caballero et al., "Distributed MIMO Antenna Architecture for Wireless-over-Fiber Backhaul with Multicarrier Optical Phase Modulation," *Opt. Fiber Commun. Conf.*, Los Angeles, CA, USA, Mar. 6–10, 2011, pp. 1–3.

[14] D. Wake, A. Nkansah, and N.J. Gomes, "Radio over Fiber Link Design for Next Generation Wireless Systems," *IEEE/OSA J. Lightw. Technol.*, vol. 28, no. 16, Aug. 2010, pp. 2456–2464.

[15] W.P. Ng et al., "Theoretical and Experimental Optimum System Design for LTE-RoF over Varying Transmission Span and Identification of System Nonlinear Limit," *IEEE Photon. J.*, vol. 4, no. 5, Oct. 2012, pp. 1560–1571.

[16] C. Liu et al., "A Novel Multi-service Small-Cell Cloud Radio

Access Network for Mobile Backhaul and Computing Based on Radio-over-Fiber Technologies," *IEEE/OSA J. Lightw. Technol.*, vol. 31, no. 17, Sept. 2013, pp. 2869–2875.

[17] D. Wake et al., "A Comparison of Radio over Fiber Link Types for the Support of Wideband Radio Channels," *IEEE/OSA J. Lightw. Technol.*, vol. 28, no. 16, Aug. 2010, pp. 2416–2422.

[18] T. Kanesan et al., "Impact of Optical Modulators in LTE RoF System with Nonlinear Compensator for Enhanced Power Budget," *Opt. Fiber Commun. Conf.*, Anaheim, CA, USA, Mar. 17–21, 2013, pp. 1–3.

[19] 3GPP TS 36.104 v. 9.1.0, *Base Station (BS) Radio Transmission and Reception: Tech. Spec. Group Radio Access Network*, *Rel. 9*, Sept. 2009.

[20] 3GPP TS 36.521-1 v. 11.2.0, *LTE; Evolved Universal Terrestrial Radio Access (E-UTRA); User Equipment (UE) Conformance Specification; Radio Transmission and Reception; Part 1: Conformance Testing*, *Tech. Spec. Group Radio Access Network*, *Rel. 11*, Sept. 2013.

[21] H. Holma and A. Toskala., "*LTE for UMTS-OFDMA and SC-FDMA Based Radio Access*," Hoboken, NJ, USA: John Wiley & Sons, Apr. 2009.

[22] V.J. Urick et al., "The Performance of Analog Photonic Links Employing Highly Compressed Erbium-Doped Fiber Amplifiers," *IEEE Trans. Microw. Theory Techn.*, vol. 54, no. 7, July 2006, pp. 3141–3145.

Seung-Hyun Cho received his BS and MS degrees in electronic materials engineering from Kwangwoon University, Seoul, Rep. of Korea, in 1997 and 1999, respectively. He received his PhD degree in materials science and engineering from Hanyang University, Seoul, Rep. of Korea, in 2010. From 1999 to 2000, he worked for Access Network Laboratory of Korea Telecom, Daejeon, Rep. of Korea. Since 2000, he has been with ETRI, where he is now a senior researcher. His current research interests are next-generation optical access networks; mobile fronthaul and backhaul networks; and optical-mobile converged access networks.

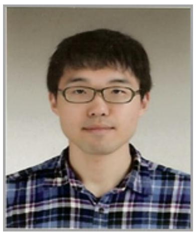

Changyo Han received his BS degree in electrical and electronic engineering from the Tokyo Institute of Technology, Japan, in 2011 and his MS degree in electrical engineering and information systems from the University of Tokyo, Japan, in 2013. In 2013, he joined ETRI. His current research interests are radio-over-fiber technology, coherent optical communication systems, and spatial multiplexing.

Hwan Seok Chung received his PhD degree in electronics engineering from the Korea Advanced Institute of Science and Technology (KAIST), Daejeon, Rep. of Korea, in 2003. In 2003, he was a postdoctoral research associate with KAIST, where he worked on a hybrid CWDM/DWDM system for a metro area network. From 2004 to 2005, he was with KDDI R&D laboratories Inc., Saitama, Japan and had engaged in research on wavelength converters and regenerators. Since 2005, he has been with ETRI, where he is currently a principal research engineer. His current research interests are mobile fronthauls, high-speed passive optical networks, and modulation formats. He served as a technical committee member at the Optical Fiber Communication Conference, Optoelectronics and Communications Conference, Conference on Optical Internet, and Photonic West. He was the recipient of the best paper award from the Optoelectronics and Communications Conference in 2000 and 2003 as well as ETRI in 2011 and 2012. He is also a senior member of IEEE.

Jong Hyun Lee received his BS, MS, and PhD degrees in electronics engineering from Sungkyunkwan University, Suwon, Rep of Korea, in 1981, 1983, and 1993, respectively. Since 1983, he has been with ETRI, where he has served as a director of both the Optical Communication Department and the Research Strategy & Planning Department. He was also an executive director of the Optical Internet Research Department. His current research interests are packet-circuit-optical converged switching systems, green Internet data center, and optical access networks.

http://dx.doi.org/10.4218/etrij.15.0115.0146